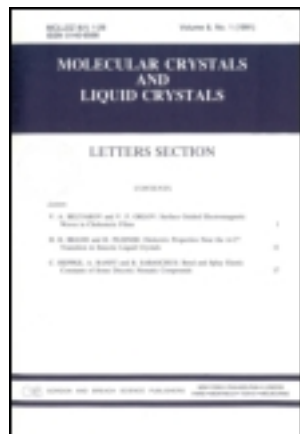


This article was downloaded by: [Moskow State Univ Bibliote]

On: 23 January 2014, At: 12:39

Publisher: Taylor & Francis

Informa Ltd Registered in England and Wales Registered Number: 1072954 Registered office: Mortimer House, 37-41 Mortimer Street, London W1T 3JH, UK



## Molecular Crystals and Liquid Crystals

Publication details, including instructions for authors and subscription information:

<http://www.tandfonline.com/loi/gmcl20>

### Synthesis and Surface Characterizations of New Banana-Shaped Liquid Crystal 4-Bromo-1,3-phenylene-bis[4-[4'-(10-undecenyloxy)-benzoyloxy]]benzoate

Cigdem Yorur-Goreci<sup>a</sup>, Fatih Cakar<sup>a</sup>, Merve Gultekin<sup>a</sup>, Ozlem Cankurtaran<sup>a</sup>, Ferdane Karaman<sup>a</sup> & Belkis Bilgin-Eran<sup>a</sup>

<sup>a</sup> Department of Chemistry, Yildiz Technical University, Istanbul, Turkey

Published online: 16 Dec 2013.

To cite this article: Cigdem Yorur-Goreci, Fatih Cakar, Merve Gultekin, Ozlem Cankurtaran, Ferdane Karaman & Belkis Bilgin-Eran (2013) Synthesis and Surface Characterizations of New Banana-Shaped Liquid Crystal 4-Bromo-1,3-phenylene-bis[4-[4'-(10-undecenyloxy)-benzoyloxy]]benzoate, Molecular Crystals and Liquid Crystals, 587:1, 28-40, DOI: [10.1080/15421406.2013.807180](http://dx.doi.org/10.1080/15421406.2013.807180)

To link to this article: <http://dx.doi.org/10.1080/15421406.2013.807180>

PLEASE SCROLL DOWN FOR ARTICLE

Taylor & Francis makes every effort to ensure the accuracy of all the information (the "Content") contained in the publications on our platform. However, Taylor & Francis, our agents, and our licensors make no representations or warranties whatsoever as to the accuracy, completeness, or suitability for any purpose of the Content. Any opinions and views expressed in this publication are the opinions and views of the authors, and are not the views of or endorsed by Taylor & Francis. The accuracy of the Content should not be relied upon and should be independently verified with primary sources of information. Taylor and Francis shall not be liable for any losses, actions, claims, proceedings, demands, costs, expenses, damages, and other liabilities whatsoever or howsoever caused arising directly or indirectly in connection with, in relation to or arising out of the use of the Content.

This article may be used for research, teaching, and private study purposes. Any substantial or systematic reproduction, redistribution, reselling, loan, sub-licensing, systematic supply, or distribution in any form to anyone is expressly forbidden. Terms & Conditions of access and use can be found at <http://www.tandfonline.com/page/terms-and-conditions>

# Synthesis and Surface Characterizations of New Banana-Shaped Liquid Crystal 4-Bromo-1,3-phenylene-bis[4-[4'-(10- undecenylloxy)-benzoyloxy]]benzoate

CIGDEM YORUR-GORECI, FATİH ÇAKAR,  
MERVE GULTEKIN, OZLEM CANKURTARAN,\*  
FERDANE KARAMAN, AND BELKIS BILGIN-ERAN

Department of Chemistry, Yildiz Technical University, Istanbul, Turkey

*A new banana-shaped liquid crystal compound, i.e., the bent-core mesogen, 4-Bromo-1,3-phenylene-bis[4-[4'-(10-undecenylloxy)-benzoyloxy]]benzoate (BPUBB), has been synthesized and characterized. Phase transition temperatures of BPUBB were determined by polarizing microscopy and differential scanning calorimetry. The inverse gas chromatography method was utilized to obtain the surface characterization of BPUBB. This compound was used as a stationary phase in the chromatographic column and nine solutes with a different chemical nature were used as eluents. The dispersive component of the surface free energy,  $\gamma_s^D$ , of studied adsorbent surface was estimated using retention times of different nonpolar organics in the infinite dilution region. The specific free energy of adsorption,  $\Delta G_A^S$ , the enthalpy of adsorption,  $\Delta H_A^S$ , and the entropy of adsorption,  $\Delta S_A^S$ , of solvents on liquid crystal were determined. The values of the  $\Delta H_A^S$  were correlated with both the donor and the acceptor numbers of the probes to quantify the acid  $K_A$  and the basic  $K_B$  parameters of the liquid crystal surface. The values obtained for the  $K_A$  and  $K_B$  parameters indicated a basic character for the surface of the BPUBB.*

**Keywords** Inverse gas chromatography; Lewis acid-base constants; liquid crystals; surface and adsorption properties; surface free energies

## Introduction

Liquid crystals have been studied for many years not only because of their technological importance but also because of their extraordinary physical properties such as dielectric and optical anisotropy, flow properties, and response to external fields [1–6].

Thermotropic liquid crystalline phases are determined by the shape of the molecules. The banana-shaped mesogens represent a new sub-field of liquid crystals. Because of the sterically induced packing of the bent molecules new smectic modifications can occur, which show new mesophases with unusual properties compared to smectic phases formed by calamitic compounds. Additionally, structural features of the new mesophases can lead to unusual physical properties [7–11].

---

\*Address correspondence to Ozlem Cankurtaran, Department of Chemistry, Yildiz Technical University, Davutpasa Campus, 34220, Istanbul, Turkey. Tel.: +902123834183. E-mail: kurtaran@yildiz.edu.tr

The surface properties of liquid crystals are very important for the performance of liquid crystal displays and devices. These properties, which is of vital importance for the alignment of the liquid crystals and thus for the appearance and operation of these devices, depends, in addition, on the solid surface–liquid crystal interactions [12]. The presence of acidic and basic centers on the molecule surface increases the specific intermolecular interactions with solvents and other molecules [13]. So it is very important to determine the surface energy and the quantity of acid–base character of compound.

Inverse gas chromatography (IGC) has become a powerful technique for evaluating the properties of solids and liquids. It provides access to several physico-chemical properties of such materials including their surface energy, phase transitions, crystallinity, acid–base characteristics, and determining of the transition temperatures of liquid crystals. In IGC, volatile compounds are influenced with the stationary phase that strongly depends on the molecular structure. Many research on IGC studies of polymers and liquid crystal polymers are present in literature [13–17]; however, the IGC studies on calamitic liquid crystal have been reported only in recent years [18–22]. According to our knowledge, there is no extant study about IGC investigation of banana-shaped liquid crystals.

In this article, we present to synthesize and characterize the surface behavior of a banana-shaped liquid crystal derived from 4-bromo resorcinol by the method of IGC. The surface free energy and acid–base characteristics of a banana-shaped liquid crystal compound were utilized through measurements of net retention volumes of several probe molecules and by use of adsorption on principle in IGC. Retentions of nine organic compounds of different chemical nature and polarity (nonpolar, donor, or acceptor) were measured in the temperature range 308.2–333.2 K. The thermodynamic parameters of adsorption, the dispersive surface energy, as well as the  $K_A$  and  $K_D$  values that describe the ability of a liquid crystal surface to act as electron acceptor or donor were calculated for banana-shaped liquid crystalline sample.

## Experimental

### *Materials and Instrumentation*

The Leco CHNS-932 Elemental Analyzer was used for micro analysis (EA). The MS spectrum for this compound was obtained using Inctectra GmbH, AMD 402.  $^1\text{H}$ - and  $^{13}\text{C}$  NMR spectra were recorded on Varian Unity 400 and Varian Gemini 200 spectrometers and sample was in solution (in  $\text{CDCl}_3$ ).

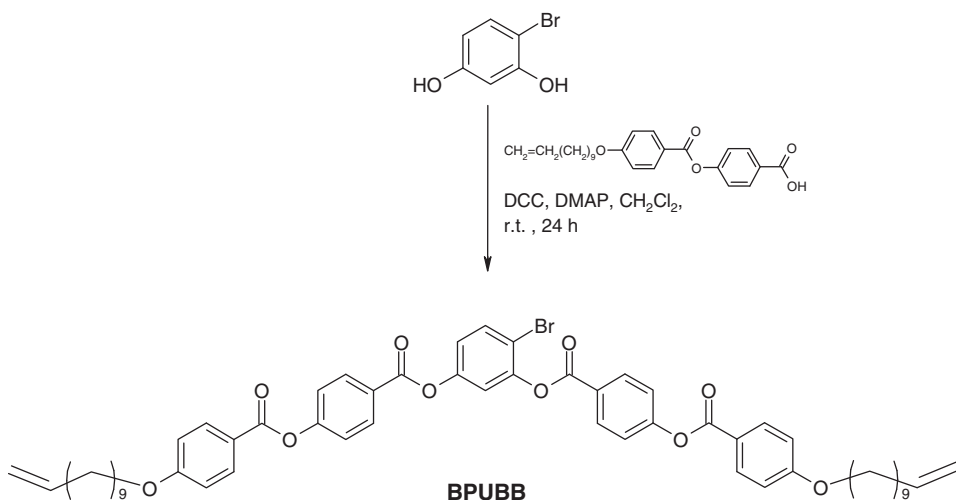
Mesomorphic properties were studied by optical microscopy using a Leitz Laborlux 12 Pol Polarizing Microscope with crossed polarizers. The microscope was connected to a Linkam TMS 600 hot stage. Transition temperatures were determined by differential scanning calorimetry (DSC) using Perkin-Elmer DSC-7.

Surface characterizations were obtained using a Hewlett-Packard 6890N model gas chromatograph with a thermal conductivity detector that was used to measure the retention time of the solvents in this study. The column was stainless steel tubing with 3.2 mm o.d. and 0.5 m in length. The **BPUBB** was coated on the support by slow evaporation of chloroform and stirring the Chromosorb-W in the **BPUBB** solution. Trace amount of solvent that was taken by Hamilton syringe as 1  $\mu\text{L}$ , poured and diluted with air three times, was injected into the chromatograph at infinite dilution. The column was conditioned at 50°C for 24 h under argon atmosphere.

The probes were high purity grade *n*-alkanes, such as *n*-heptane (Hp), *n*-octane (O), *n*-nonane (N), and decane (D), and other acidic, basic, and amphoteric probes such as tetrahydrofuran (THF, basic), dichloromethane (DCM, acidic), chloroform (TCM, acidic), acetone (ACe, amphoteric), and ethyl acetate (EA, amphoteric) used without further purification. All the studied solvents and support materials such as Chromosorb-W (AW-DMCS-treated, 80/100 mesh) were supplied from Merck AG. Inc. Silane-treated glass wool used to plug the ends of the column was obtained from Alltech Associates, Inc.

### Synthesis and Characterization of BPUBB

**BPUBB** were obtained by following the synthetic procedure [23, 34] described in Scheme 1 by DCC coupling of the 4-[4-(undec-10-enyloxy)benzoyloxy]benzoic acid and the commercially available 4-bromo-1,3-benzene diol. The synthesis and the analytical data of the 4-[4-(undec-10-enyloxy)benzoyloxy]benzoic acid were reported in literature [24].



**Scheme 1.** Synthesis of **BPUBB**.

A mixture of 4-bromo-1,3-benzene diol (4 mmol), 4-[4-(undec-10-enyloxy)benzoyloxy]benzoic acid (2 mmol), DCC (0.62 g, 3 mmol), and DMAP (50 mg) in dry DCM (70 mL) was stirred at room temperature under argon for 24 h. The mixture was filtered, the solid was washed with dichloromethane, and the filtrate was evaporated to dryness. The product was purified by column chromatography (silica gel, elution with  $\text{CHCl}_3$ ).

White crystals, 61% yield (found: C, 69.2; H, 6.5;  $\text{C}_{56}\text{H}_{61}\text{BrO}_{10}$  requires C, 69.1; H, 6.3).  $^1\text{H}$  NMR (400 MHz,  $\text{CDCl}_3$ , TMS):  $\delta$  8.31 (d,  $J \approx 8.7$  Hz; 2 Ar-H), 8.24 (d,  $J \approx 8.7$  Hz; 2 Ar-H), 8.14 (d,  $J \approx 8.9$  Hz; 2 Ar-H), 8.13 (d,  $J \approx 8.9$  Hz; 2 Ar-H), 7.69 (d,  $J \approx 8.7$  Hz; 1 Ar-H), 7.36 (d,  $J \approx 8.7$  Hz; 2 Ar-H), 7.35 (d,  $J \approx 8.7$  Hz; 2 Ar-H), 7.29 (d,  $J \approx 2.7$  Hz; 1 Ar-H), 7.10 (dd,  $J \approx 8.7$  Hz,  $J \approx 2.7$  Hz; 1 Ar-H), 6.97 (d,  $J \approx 8.9$  Hz; 4 Ar-H), 5.85–5.75 (m; 2H,  $\text{CH}_2=\text{CH}$ ), 5.01–4.90 (m; 4H,  $\text{CH}=\text{CH}_2$ ), 4.04 (t;  $J \approx 6.6$  Hz; 4H,  $2\text{OCH}_2$ ), 2.06–2.00 (m; 4H,  $\text{H}_2\text{C}=\text{CH}-\text{CH}_2$ ), 1.85–1.78 (m; 4H,  $\text{OCH}_2\text{CH}_2$ ), 1.53–1.24 (m; 24H, 12  $\text{CH}_2$ ).  $^{13}\text{C}$  NMR (125 MHz,  $\text{CDCl}_3$ ):  $\delta$  (ppm) = 164.08, 163.72, 163.63 (3s; 4CO), 163.03, 155.61, 155.53, 150.42, 148.69, 128.71, 126.23, 126.01, 120.92, 120.91 (10s; 11 Ar-C), 139.05 (d; 2  $\text{CH}_2=\text{CH}$ ), 133.35, 132.32, 132.00, 131.78, 130.73, 122.13, 122.10, 120.91, 117.84, 114.40 (10d; 19 Ar-CH), 114.07 (t; 2  $\text{CH}=\text{CH}_2$ ), 68.43

(t; 2 OCH<sub>2</sub>), 33.85, 29.77, 29.56, 29.48, 29.40, 29.18, 29.01, 26.06 (8t; 16 CH<sub>2</sub>). MS (EI) m/z = 393 (6) [M<sup>+</sup>-C<sub>31</sub>H<sub>32</sub>BrO<sub>6</sub>], 273 (100) [M<sup>+</sup>-C<sub>38</sub>H<sub>36</sub>BrO<sub>8</sub>], 121 (67) [C<sub>9</sub>H<sub>13</sub>].

### *Inverse Gas Chromatography Theory for Surface Characterization*

The interaction between the liquid crystal and the probe is quantified by the retention time for the particular probe. The adsorbate retention time,  $t_R$ , is dependent upon the carrier gas flow rate that is used in the experiment. Thus, a net retention volume,  $V_N$ , is determined by the equation:

$$V_N = Q \cdot J \cdot (t_R - t_A) \cdot T / (T_f), \quad (1)$$

where  $t_A$  is the retention time of air,  $Q$  is volumetric flow rate measured at column outlet and at ambient temperature  $T_f$  (K),  $T$  is the column temperature (K), and  $J$  is James-Martin gas compressibility correction factor [13, 25, 26]. The interactions experienced between an adsorbate and an adsorbent can consist of two components-specific and dispersion forces [27]. Dispersion forces, also known as London forces, are present between all molecules, regardless of their identity. Specific forces generally rely on some compatibility between the structures of the interacting molecules, either physically or electronically.

Intermolecular interactions in the adsorbate/adsorbent system may be dispersive and specific, which corresponds to the dispersive,  $\gamma_S^D$ , and the specific,  $\gamma_S^S$ , components of the free surface energy,  $\gamma_S$ , of the adsorbent:

$$\gamma_S = \gamma_S^D + \gamma_S^S, \quad (2)$$

The dispersive surface energy is a very important parameter that describes the material surface to establish nonpolar interactions with other substances. The dispersive component of surface energy is determined using both Dorris-Gray [28] and Fowkes [29] methods. According to Dorris-Gray,  $\gamma_S^D$  is described by the following equation:

$$\Delta G_{A[CH_2]} = 2N_A a_{[CH_2]} \sqrt{\gamma_S^D \gamma_{L[CH_2]}}, \quad (3)$$

where  $\Delta G_{A[CH_2]}$  is the adsorption free energy of one methylene group,  $N_A$  is Avogadro's number,  $a_{[CH_2]}$  is the cross-sectional area of an adsorbed methylene group, and  $\gamma_{L[CH_2]}$  is the surface free energy of a solid material constituted by methylene groups only, such as polyethylene [ $\gamma_{L[CH_2]} = 35.6 + 0.058(293.2 - T)$ ,  $T$  is the working temperature in K]. The adsorption free energy of one methylene group is calculated by the following equation:

$$\Delta G_{A[CH_2]} = -RT \ln \left( \frac{V_{N,n}}{V_{N,n+1}} \right), \quad (4)$$

where  $R$  is the ideal gas constant,  $T$  is the column temperature, and  $V_{N,n}$  and  $V_{N,n+1}$  are the retention volumes of two  $n$ -alkanes having  $n$  and  $n+1$  carbon atoms in their chain.

The plot of the  $RT \ln V_N$  values of  $n$ -alkanes versus the number of carbon atoms of  $n$ -alkanes is linear. The slope of the straight line is equal to the free energy of adsorption of a methylene group,  $\Delta G_{A[CH_2]}$ .

Thus using Eqs. (3) and (4) and the experimentally determined values of  $V_{N,n}$  and  $V_{N,n+1}$ , the dispersion component of the surface free energy,  $\gamma_S^D$ , may be calculated.

**Table 1.** Values of  $a(\gamma_L^D)^{0.5}$  for the selected  $n$ -alkane solvents

| Probe | $a(\times 10^{-10} \text{ m}^2)$ | $\gamma_L^D (\text{mJ/m}^2)$ | $a(\gamma_L^D)^{0.5} (\text{m}^2 (\text{mJ/m}^2)^{0.5})$ |
|-------|----------------------------------|------------------------------|--|
| Hp    | 57.0                             | 20.3                         | $2.57 \times 10^{-18}$                                   |
| O     | 62.8                             | 21.3                         | $2.90 \times 10^{-18}$                                   |
| N     | 69.0                             | 22.7                         | $3.28 \times 10^{-18}$                                   |
| D     | 75.0                             | 23.4                         | $3.63 \times 10^{-18}$                                   |

The free energy of adsorption,  $\Delta G_A$ , is related to the net retention volume as follows [30]:

$$\Delta G_A = -RT \ln(V_N) + K, \quad (5)$$

where  $T$  is the column temperature and  $K$  is a constant for a given column.

According to Fowkes's method,  $\gamma_S^D$  is related to net retention volume by the following relation [31]:

$$-\Delta G_A = RT \ln(V_N) = 2Na(\gamma_S^D)^{0.5}(\gamma_L^D)^{0.5} + K'', \quad (6)$$

where  $\gamma_L^D$  is the dispersive component of the surface free energy of adsorbent.

Thus for a series of  $n$ -alkane probes, a plot of  $RT \ln V_N$  against  $a(\gamma_L^D)^{0.5}$  will give a slope of  $2N(\gamma_S^D)^{0.5}$ . Values of  $a(\gamma_L^D)^{0.5}$  are found in the literature [29, 31]. The values of  $a(\gamma_L^D)^{0.5}$  for  $n$ -alkanes are presented in Table 1.

The specific component of the free energy is determined from the  $n$ -alkane plot of  $RT \ln V_N$  against  $a(\gamma_L^D)^{0.5}$ . The distance between the ordinate values of the polar probe datum point and the  $n$ -alkane reference line gives the specific component of the surface free energy,  $-\Delta G_A^S$ . An equation may be written for this procedure:

$$-\Delta G_A^S = RT \ln \left( \frac{V_{N,n}}{V_{N,ref}} \right), \quad (7)$$

where  $V_{N,n}$  and  $V_{N,ref}$  are the retention volume for the polar probe and the retention volume for the  $n$ -alkanes' reference line, respectively.

Values of  $a(\gamma_L^D)^{0.5}$ , the Gutmann's modified acceptor number,  $AN^*$ , and donor number,  $DN^*$ , of the polar probes used in this study are presented in Table 2 [32, 33].

The adsorption of a polar probe onto the adsorbent surface leads to a change in the enthalpy of the system and the entropy of the system. These factors are related to the

**Table 2.** Values of  $a(\gamma_L^D)^{0.5}$ ,  $DN$ , and  $AN^*$  for the selected polar solvent

| Probe | $a(\times 10^{-10} \text{ m}^2)$ | $\gamma_L^D (\text{mJ/m}^2)$ | $a(\gamma_L^D)^{0.5} (\text{m}^2 (\text{mJ/m}^2)^{0.5})$ | $AN^* (\text{kJ/mol})$ | $DN (\text{kJ/mol})$ |
|-------|----------------------------------|------------------------------|--|------------------------|----------------------|
| DCM   | 31.5                             | 27.6                         | $1.65 \times 10^{-18}$                                   | 16.4                   | 0.0                  |
| TCM   | 44.0                             | 25.9                         | $2.24 \times 10^{-18}$                                   | 22.7                   | 0.0                  |
| THF   | 45.0                             | 22.5                         | $2.13 \times 10^{-18}$                                   | 2.1                    | 84.0                 |
| ACe   | 42.5                             | 16.5                         | $1.73 \times 10^{-18}$                                   | 10.5                   | 71.4                 |
| EA    | 48.0                             | 19.6                         | $2.13 \times 10^{-18}$                                   | 6.3                    | 71.8                 |

specific component of the surface free energy by the equation:

$$\Delta G_A^S = \Delta H_A^S - T \Delta S_A^S \quad (8)$$

Here,  $\Delta H_A^S$  is the adsorption enthalpy by Lewis acid–base interactions,  $\Delta S_A^S$  is the adsorption entropy Lewis acid–base interactions, and  $T$  is the column temperature. By plotting  $-\Delta G_A^S/T$  values as a function of the reciprocal temperature  $T^{-1}$ ,  $\Delta H_A^S$  and  $\Delta S_A^S$  can be calculated for each polar probe corresponding to the equation:

$$\Delta G_A^S/T = \Delta H_A^S/T - \Delta S_A^S \quad (9)$$

The enthalpies of specific interactions between the examined surface and the polar solute are related to the acid or basic character through the equation:

$$-\Delta H_A^S/AN^* = K_A \cdot DN/AN^* + K_D, \quad (10)$$

where  $DN$  and  $AN^*$  are Gutmann's donor and modified acceptor numbers, respectively, whereas  $K_A$  and  $K_D$  are indicators reflecting Lewis acidity and basicity of a solid surface. Consequently,  $K_A$  and  $K_D$  can be determined by the slope and intercept, respectively, of the straight line obtained by plotting  $-\Delta H_A^S/AN^*$  versus  $DN/AN^*$ . The ratio  $K_D/K_A$  provides an empirical basis for the classification of a surface with respect to acidity–basicity. At  $K_D/K_A > 1$  the surface is considered to be basic, while  $K_D/K_A < 1$  the surface is considered to be acidic.

## Results and Discussion

### Liquid Crystalline Properties

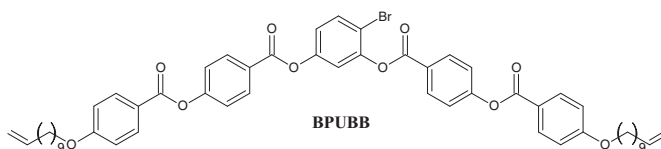
The mesomorphic properties of the obtained new “bent-core” compound **BPUBB** were investigated by polarized light microscopy (PM) and DSC.

**BPUBB** was found to exhibit thermotropic nematic mesophase within a wide range of temperature. For this compound, the transition of crystal–nematic phase at 65.2°C occurred while the nematic–isotropic phase transition occurred at 109.1°C. The transition temperatures, corresponding enthalpy values, and the typical texture of the nematic mesophase of **BPUBB** are given in Fig. 1. On cooling from the isotropic phase, the sample is macroscopically aligned in the nematic phase.

A preliminary insight into the structure–property relationships of bent-core molecules revealed that the mesophase behavior is strongly influenced by nature of terminal substituents in the bent core. In previous years, the halogen-free structural analogs of **BPUBB** have been reported that they exhibited layered mesophases such as smectic C [34, 35]. In our study, the presence of bulky bromine atom led to transition from layered mesophases to nematic phase. Because the repulsion between the bulky bromine substituent in **BPUBB** and adjacent ester linkages leads to cause a rotation on the wing of the bent molecule and increases in the bending angle, therefore mesomorphic behavior of the compound changes, which occurs in non-ordered mesophase [36].

### Surface Characterizations of BPUBB by IGC

The sorption properties of **BPUBB** were investigated at infinite dilution conditions by IGC between 308.2 K and 333.2 K. The net retention volumes,  $V_N$ , of the nonpolar, polar, and



Cr 65.2 [23.4] N 109.1 [1.4] Iso

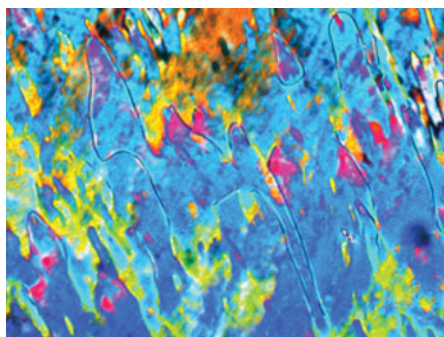


**Figure 1.** Mesophase texture exhibited (in cooling) by **BPUBB** in nematic phase at 76°C and mesophase transition temperatures (Perkin-Elmer DSC-7; heating rates 10 K min<sup>-1</sup>; enthalpy value given behind the phase transition temperatures in italics in square parentheses; abbreviations: Cr = crystalline, N = nematic phase, and Iso = isotropic liquid phase).

amphoteric probes on the **BPUBB** were obtained using Eq. (1). A plot of  $RT \ln V_N$  versus  $1/T$  for studied solutes is drawn in Figs. 2 and 3, respectively.

The dispersive component of the free surface energy of **BPUBB** was determined using both Dorris-Gray and Fowkes methods. Dispersive surface free energy of the stationary phase can be obtained using the net retention volume of the *n*-alkane probes. According to the theory, only dispersive interaction will take place between the *n*-alkanes and the stationary phase. Thus at constant temperatures, for a series of alkane probes, a plot  $RT \ln V_N$  versus the number of carbon atoms should give a straight line from which  $\Delta G_{A[CH_2]}$  can be found.  $\gamma_S^D$  was calculated from Eq. (3). The results of  $\Delta G_{A[CH_2]}$ ,  $\gamma_{L[CH_2]}$  and  $\gamma_S^D$  are given in Table 3.

**Table 3.** The adsorption free energy of one methylene group,  $\Delta G_{A[CH_2]}$ , the surface free energy of a solid material constituted by methylene groups,  $\gamma_{L[CH_2]}$ , and dispersion component of surface free energy,  $\gamma_S^D$ , values calculated by Dorris-Gray method for **BPUBB** determined at studied temperatures

| T(K)  | $\gamma_{L[CH_2]}$ (mJ/m <sup>2</sup> ) | $\Delta G_{A[CH_2]}$ (10 <sup>6</sup> mJ/mol) | $\gamma_S^D$ (mJ/m <sup>2</sup> ) |
|-------|---|---|-----------------------------------|
| 308.2 | 34.73                                   | -2.56   | 36.05                             |
| 313.2 | 34.44                                   | -2.51   | 34.93                             |
| 318.2 | 34.15                                   | -2.43   | 33.24                             |
| 323.2 | 33.86                                   | -2.42   | 32.99                             |
| 328.2 | 33.57                                   | -2.40   | 32.77                             |
| 333.2 | 33.28                                   | -2.38   | 32.55                             |



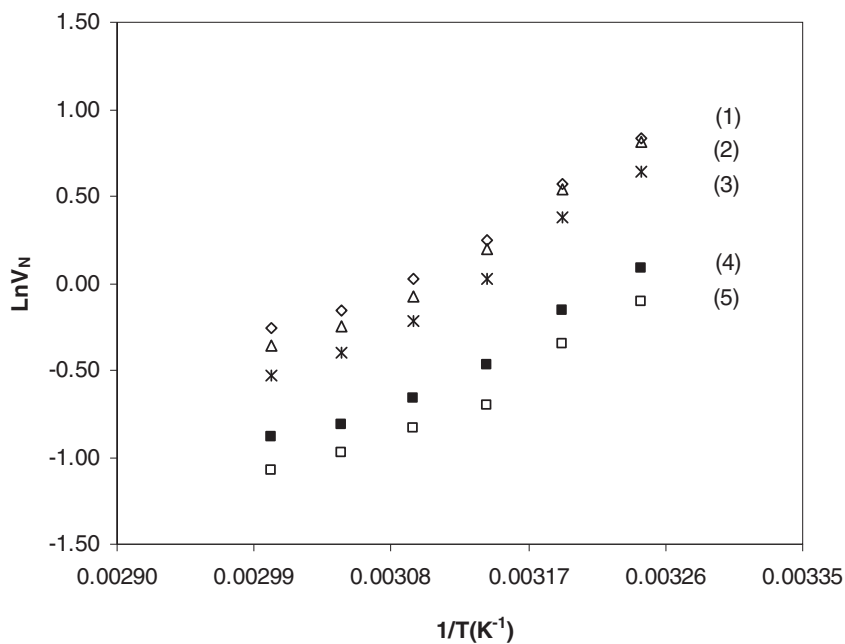


**Figure 2.** The net retention volumes of THF (1), TCM (2), EA (3), DCM (4), and ACe (5) on BPUBB.

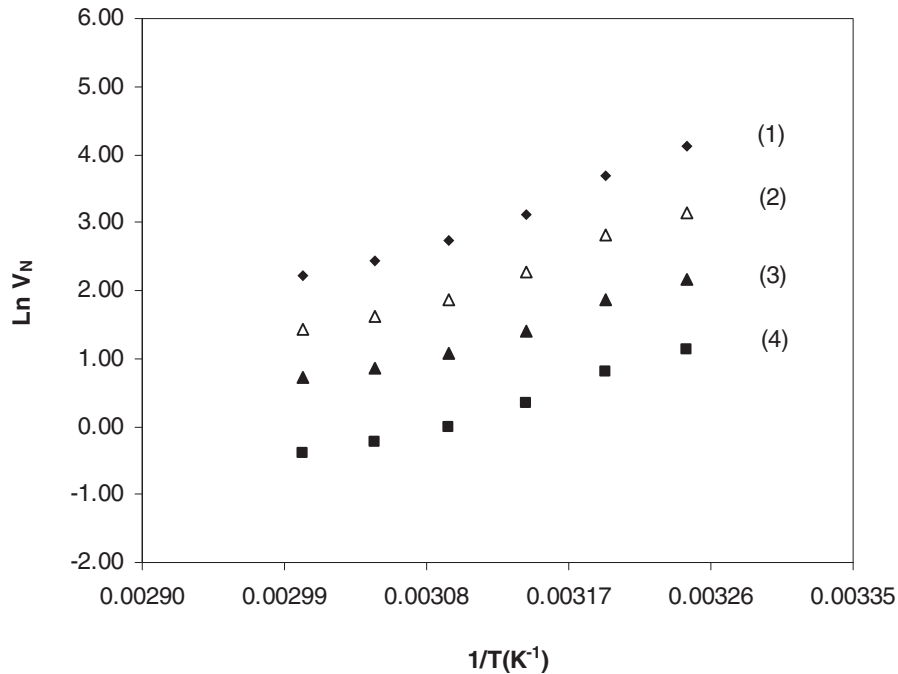


**Figure 3.** The net retention volumes of D (1), N (2), O (3), and Hp (4) on BPUBB.

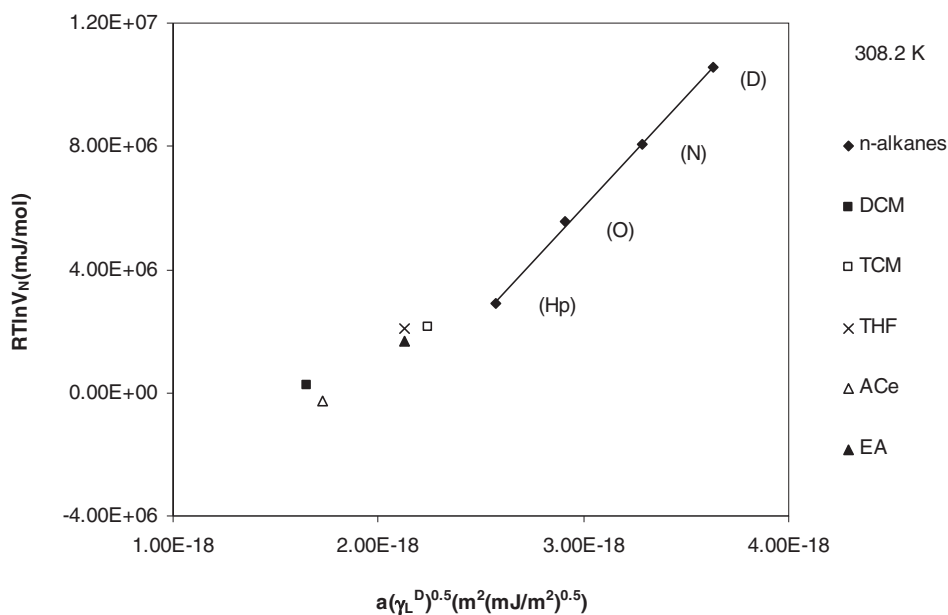


**Figure 4.** A plot of  $RT \ln V_N$  versus  $a(\gamma_L^D)^{0.5}$  for  $n$ -alkanes and polar probes on **BPUBB** at 308.2 K.

As observed from Table 4, the dispersive component of surface free energy of **BPUBB** decreases with the increase of temperature while the decrease is almost linear in the investigated temperature range.

The free energy of adsorption,  $\Delta G_A$ , for the  $n$ -alkanes and five polar solvents were calculated from Fowkes method using Eqs. (5) and (6) in the temperature range 308.2 K and 333.2 K. A plot of  $RT \ln V_N$  versus  $a(\gamma_L^D)^{0.5}$  for  $n$ -alkanes and polar solutes is drawn as an example for the data measured at 308.2 K in Fig. 4. In this figure, a straight-line plot is obtained for  $n$ -alkanes series and the slope of this straight line was used to obtain  $\gamma_S^D$ . The variation in  $\gamma_S^D$  with temperature is shown in Fig. 4.

Figure 5 reports that the  $\gamma_S^D$  values of **BPUBB** decrease with increase in the temperature. The values of  $\gamma_S^D$  calculated according to Dorris-Gray and Fowkes approaches are very close to each other at the studied temperature ranges.

**Table 4.** The variation of free energy of specific interactions,  $\Delta G_A^S$  (kJ/mol), between **BPUBB** and polar probes for studied temperatures

| T(K)  | DCM  | TCM  | THF  | ACe  | EA   |
|-------|------|------|------|------|------|
| 308.2 | 3.88 | 1.55 | 2.29 | 2.79 | 1.84 |
| 313.2 | 3.85 | 1.58 | 2.27 | 2.77 | 1.86 |
| 318.2 | 3.95 | 1.83 | 2.44 | 2.81 | 1.99 |
| 323.2 | 4.24 | 2.09 | 2.56 | 3.24 | 2.18 |
| 328.2 | 4.33 | 2.15 | 2.63 | 3.34 | 2.24 |
| 333.2 | 4.47 | 2.26 | 2.70 | 3.39 | 2.22 |

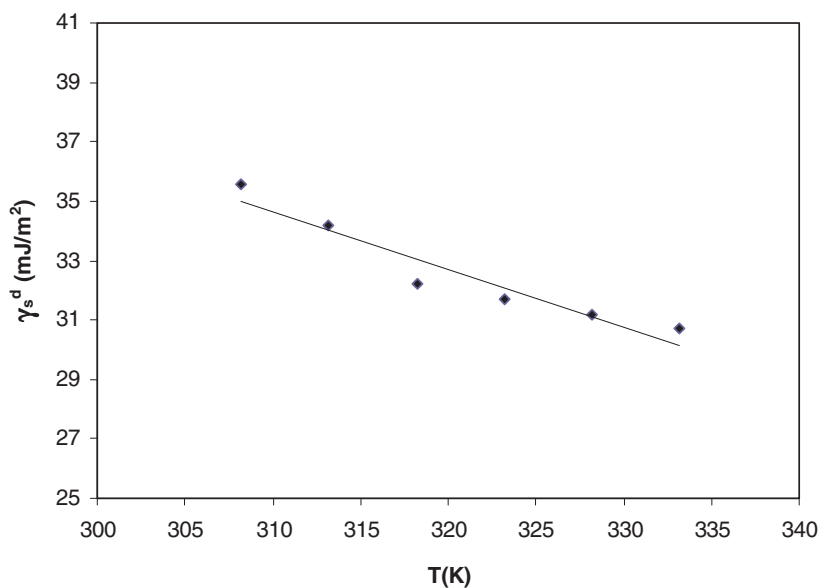


**Figure 5.** Variation of dispersive component of surface free energy,  $\gamma_s^D$ , with the temperature for BPUBB.

The specific component of the surface free energy,  $-\Delta G_A^S$ , is calculated using the difference between the calculated value of  $RT \ln V_N$  and that which was derived using Eq. (7) of the linear fit of the *n*-alkane reference line. The variation of free energy of specific interactions,  $\Delta G_A^S$ , between BPUBB and polar probes for different temperature is given in Table 4.

It was observed that the temperature increases as the value of  $\Delta G_A^S$  generally increases. The  $\Delta G_A^S$  values of polar probes increase in the following order: TCM < EA < THF < ACe < DCM.

By plotting the values of  $-\Delta G_A^S/T$  against  $1/T$ ,  $\Delta H_A^S$  the enthalpy and  $\Delta S_A^S$  the entropy of adsorption were determined for each polar probe.  $\Delta H_A^S$  was determined from the slope and  $\Delta S_A^S$  was determined from the intercept of the linear regression applied. The values of the enthalpy of adsorption and of the entropy of adsorption for polar probes are presented in Table 5.

**Table 5.** Values of the enthalpy,  $-\Delta H_A^S$ , and entropy,  $\Delta S_A^S$ , of adsorption on BPUBB for the polar probes

| Probe | $-\Delta H_A^S$ (kJ/mol) | $\Delta S_A^S \cdot 10^3$ (kJ/molK) |
|-------|--------------------------|-------------------------------------|
| DCM   | 4.42                     | 5.30                                |
| TCM   | 8.31                     | 3.78                                |
| THF   | 3.45                     | 5.03                                |
| ACe   | 6.31                     | 4.22                                |
| EA    | 3.88                     | 4.43                                |

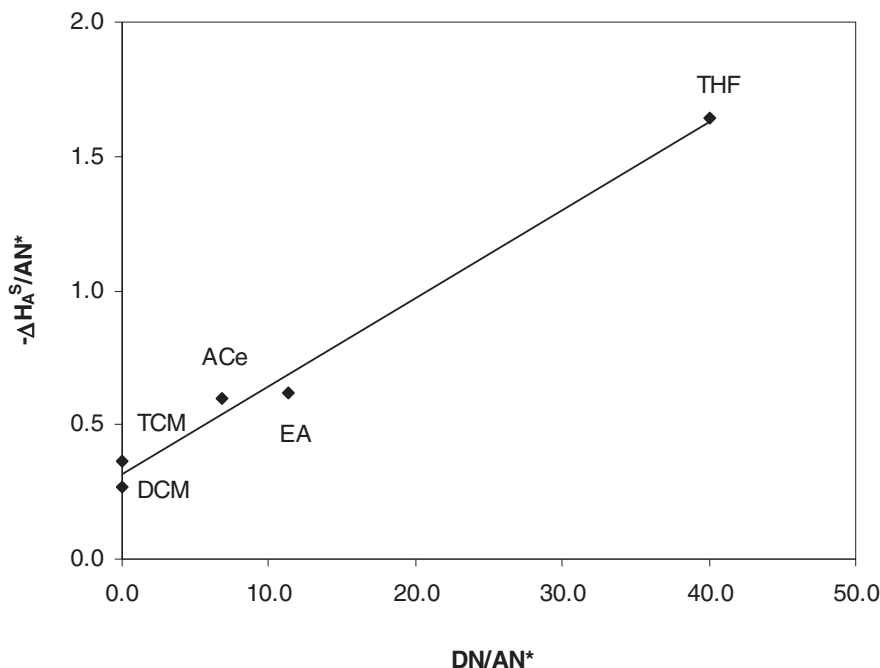


**Figure 6.** The plot of  $-\Delta H_A^S/AN^*$  versus  $DN/AN^*$ .

The value of  $\Delta H_A^S$  indicates the strength of the interaction between the probe and the surface of the BPUBB. The TCM probe presents the highest value of  $-\Delta H_A^S$  among all probes, the amphoteric probe (ACe) follows an acidic probe (DCM) and amphoteric probe (EA), and the lowest value of  $-\Delta H_A^S$  is observed for the basic probe (THF). This order suggests that the BPUBB has a basic nature.

By plotting  $-\Delta H_A^S/AN^*$  versus  $DN/AN^*$ ,  $K_A$  and  $K_D$  can be determined from the slope and intercept of the straight line (see Fig. 6).

The overall acid/base character of **BPUBB** can be evaluated from the  $K_D/K_A$  ratio.  $K_A$  and  $K_D$  parameters reflecting the ability of the examined surface to act as an electron acceptor and donor, respectively, were calculated using the specific interaction contribution to the adsorption enthalpy of the selected probe molecules. Values of  $K_D/K_A$  of greater than 1 mean a basic nature on a solid surface, and values of less than 1 imply an acidic nature. The values of  $K_A$  and  $K_D$  are found to be 0.033 and 0.316, respectively, and the ratio of  $K_D/K_A$  is equal to 9.63. According to this value, the surface of **BPUBB** exhibits a basic character between 308.2 K and 333.2 K.

## Conclusions

We synthesized, investigated, and characterized liquid crystal properties of a five-ring bent-core mesogen derived from 4-bromo resorcinol. The mesophase behavior has been studied using PM and DSC. The results of these investigations determined that nematic mesophase was observed for new **BPUBB** in wide range.

IGC at infinite dilution, as the chosen method, was used to determine the adsorption properties, and surface and Lewis acid–base characteristics of **BPUBB**. The  $\gamma_s^D$  values

of **BPUBB** change range from  $32.55 \text{ mJ m}^{-2}$  to  $36.05 \text{ mJ m}^{-2}$  (Dorris-Gray approach) from  $30.70 \text{ mJ m}^{-2}$  to  $35.56 \text{ mJ m}^{-2}$  (Fowkes approach).  $\gamma_s^D$  values from both calculation methods decrease linearly with increase of temperature in the range 308.2–333.2 K. **BPUBB** is a basic liquid crystal as confirmed by the values of  $K_D/K_A$  ratio and the specific components of the enthalpy.

Therefore, it was shown that IGC gives reasonable information about dispersive and acid–base properties of **BPUBB** surfaces.

## Acknowledgment

This research has been supported by the Yildiz Technical University Scientific Research Projects Coordination Department.

## References

- [1] Sen, N. (2000). *Curr. Sci. India*, 79, 1417.
- [2] Canli, N. Y., Yakuphanoglu, F., & Bilgin-Eran, B. (2009). *Optoelectron. Adv. Mat.*, 3, 731.
- [3] Canli, N. Y., Yakuphanoglu, F., Yasa, O., & Bilgin-Eran, B. (2010). *Optoelectron. Adv. Mat.*, 4, 821.
- [4] Manohar, R., Pandey, K. K., Srivastava, A. K., Misra, A. K., & Yadav, S. P. (2010). *J. Phys. Chem. Solids*, 71, 1311.
- [5] Lucchetti, L., Fabrizio, M. D., Francescangeli, O., & Simoni, F. (2002). *J. Nonlin. Opt. Phys. Mater.*, 11, 13.
- [6] Koccar, K., & Muscovic, I. (2003). *Liq. Cryst. Today*, 12, 3.
- [7] Niori, T., Sekine, F., Watanabe, J., Furukawa, T., & Takezoe, H. (1996). *J. Mater. Chem.*, 6, 1231.
- [8] Tamba, M. G., Kosata, B., Pelz, K., Diele, S., Pelzl, G., Vakhovskaya, Z., Kresse, H., & Weissflog, W. (2006). *Soft Matter*, 2, 60.
- [9] Bilgin-Eran, B., Tschierske, C., Diele, S., & Baumeister, U. (2006). *J. Mater. Chem.*, 16, 1145.
- [10] Pelzl, G., Diele, S., & Weissflog, W. (1999). *Adv. Mater.*, 11, 707.
- [11] Reddy, R. A., & Tschierske, C. (2006). *J. Mater. Chem.*, 16, 907.
- [12] Komitov, L., & Ichimura, K. (2001). *Mol. Cryst. Liq. Cryst.*, 360, 161.
- [13] Cakar, F., Yazici, O., Sakar, D., Cankurtaran, O., & Karaman, F. (2011). *Optoelectron. Adv. Mat.*, 5, 821.
- [14] Nastasovi, A. B., & Onjia, A. E. (2007). *J. Serb. Chem. Soc.*, 72, 403.
- [15] Price, G. J., Hickling, S. J., & Shillcock, I. M. (2002). *J. Chromatogr. A*, 969, 193.
- [16] Price, G. J., & Shillcock, I. M. (2002). *J. Chromatogr. A*, 964, 199.
- [17] Kunaver, M., Zadnik, J., Planinsek, O., & Srcic, S. (2004). *Acta Chim. Slov.*, 51, 373.
- [18] Ocak, H., Sakar, D., Cakar, F., Cankurtaran, O., Bilgin-Eran, B., & Karaman, F. (2008). *Liq. Cryst.*, 35, 1351.
- [19] Ocak, H., Yazici, O., Bilgin-Eran, B., Cankurtaran, O., & Karaman, F. (2008). *Optoelectron. Adv. Mat.*, 2, 303.
- [20] Yasa-Sahin, O., Yazici, O., Karaagac, B., Sakar, D., Cankurtaran, O., Bilgin-Eran, B., & Karaman, F. (2010). *Liq. Cryst.*, 37, 1111.
- [21] Yazici, O., Ocak, H., Yasa-Sahin, O., Sakar, D., Cankurtaran, O., Karaman, F., & Bilgin-Eran, B. (2012). *Liq. Cryst.*, 37, 1421.
- [22] Sesigur, F., Sakar, D., Yasa-Sahin, O., Ocak, H., Cankurtaran, O., Bilgin-Eran, B., & Karaman, F. (2012). *Liq. Cryst.*, 39, 87.
- [23] Reddy, R. A., Baumeister, U., Keith, C., Hahn, H., Lang, H., & Tschierske, C. (2007). *Soft Matter*, 3, 558.
- [24] Kozmik, V., Kovářová, A., Kuchař, M., Svoboda, J., Novotná, V., Glogarová, M., & Kroupa, J. (2006). *Liq. Cryst.*, 33, 41.

- [25] Conder, J. R., & Young, C. L. (1979). *Physicochemical Measurement by Gas Chromatography*, Wiley-Interscience: New York.
- [26] Papadopoulou, S. K., Dritsas, G., Karapanagiotis, I., Zuburtikudis, I., & Panayiotou, C. (2010). *Eur. Polym. J.*, 46, 202.
- [27] Kiselev, A. V. (1965). *Discuss Faraday Soc.*, 40, 205.
- [28] Dorris, G. M., & Gray, D. G. (1980). *J. Colloid Interf. Sci.*, 77, 353.
- [29] Riddle, L. F., & Fowkes, F. M. (1990). *J. Am. Chem. Soc.*, 112, 3259.
- [30] Mukhopadhyay, P., & Schreiber, H. P. (1995). *Colloid. Surf. A*, 100, 47.
- [31] Kamdem, D. P., Bose, S. K., & Luner, P. (1993). *Langmuir*, 9, 3039.
- [32] Santos, J. M. R. C. A., & Guthrie, J. T. (2005). *Mat. Sci. Eng. R.*, 50, 79.
- [33] Santos, J. M. R. C. A., & Guthrie, J. T. (2005). *J. Chromatogr. A*, 1070, 147.
- [34] Fodor-Csorba, K., Vajda, A., Galli, G., Jákl, A., Demus, D., Holly, S., & Gács-Baitz, E. (2002). *Macromol. Chem. Phys.*, 203, 1556.
- [35] Vakhovskaya, Z., Weissflog, W., Friedemann, R., & Kresse, H. (2007). *Phase Transit.*, 80, 705.
- [36] Upadhyaya, K., Gude, V., Mohiuddin, G., & Nandiraju, R. V. S. (2013). *Beilstein J. Org. Chem.*, 9, 26.